# Histone Deacetylase Inhibitors Suppress the Inducibility of Nuclear Factor-κB by Tumor Necrosis Factor-α Receptor-1 Down-regulation

**Gabriele Imre, Volker Gekeler, Astrid Leja, Thomas Beckers, and Markus Boehm**

Therapeutic Area Oncology, ALTANA Pharma AG, Konstanz, Germany

## Abstract

**Recently, the inhibition of histone deacetylase (HDAC) enzymes has attracted attention in the oncologic community as a new therapeutic opportunity for hematologic and solid tumors including non–small cell lung cancer (NSCLC). In hematologic malignancies, such as diffuse large B-cell lymphoma, the HDAC inhibitor (HDI), suberoylanilide hydroxamic acid (SAHA), has recently entered phase II and III clinical trials. To further advance our understanding of their action on tumor cells, we investigated the possible effect of HDI treatment on the functionality of the nuclear factor-κB (NF-κB) pathway in NSCLC. We found that in the NSCLC cell lines, A549 and NCI-H460, the NF-κB pathway was strongly inducible, for example, by stimulation with tumor necrosis factor-α (TNF-α). Incubation of several NSCLC cell lines with HDIs resulted in greatly reduced gene expression of TNF-α receptor-1. HDI-treated A549 and NCI-H460 cells down-regulated TNF-α receptor-1 mRNA and protein levels as well as surface exposure, and consequently responded to TNF-α treatment with reduced IKK phosphorylation and activation, delayed IκB-α phosphorylation, and attenuated NF-κB nuclear translocation and DNA binding. Accordingly, stimulation of NF-κB target gene expression by TNF-α was strongly decreased. In addition, we observed that SAHA displayed antitumor efficacy *in vivo* against A549 xenografts grown on nude mice. HDIs, therefore, might beneficially contribute to tumor treatment, possibly by reducing the responsiveness of tumor cells to the TNF-α-mediated activation of the NF-κB pathway. These findings also hint at a possible use of HDIs in inflammatory diseases, which are associated with the overproduction of TNF-α, such as rheumatoid arthritis or Crohn's disease.** (Cancer Res 2006; 66(10): 5409-18)

## Introduction

Histone deacetylases (HDACs) regulate the acetylation status of histones at prominent amino-terminal lysine residues, and their inhibitors have recently inspired great interest in the cancer research community as a possible treatment option for solid and hematologic tumors (reviewed in refs. 1–5). Currently available HDAC inhibitors (HDIs) fall into six structural classes (1), and suberoylanilide hydroxamic acid (SAHA, ref. 6) is a prototype of the hydroxamate class that inhibits class I and class II HDAC enzymes with similar potency. The basic concept is that inhibition of HDAC enzymes relieves gene repression by inducing the hyperacetylation of core histone proteins, and indeed, many studies have shown altered gene expression upon treatment of tumor cells with HDIs (7–9). Nevertheless, over the last few years, it has also become clear that HDIs not only cause a change in the histone acetylation status, but are also able to influence the acetylation status of a number of other proteins important for tumor formation and proliferation, such as p53, α-tubulin, nuclear receptors, Hsp90, signal transducer and activator of transcription family members, such as Stat3 (reviewed in ref. 10), and subunits of nuclear factor-κB (NF-κB; refs. 11–13).

Here, we focused on determining the effect of HDIs on the NF-κB signaling pathway because its activation is a most prominent route chosen by cells to evade apoptosis and to respond to stress conditions caused, e.g., by cytostatic anticancer agents (reviewed in ref. 14). NF-κB exerts its actions by binding to decameric κB sites in the promoter regions of genes that can be grouped as anti-apoptotic, proangiogenic, or proinflammatory. Besides regulating cellular homeostasis, NF-κB can also influence cell motility by activating adhesion or matrix remodeling genes, such as MMP9 and vimentin (15).

The most common NF-κB isoforms are heterodimers composed of p65 and p50, which have a role in inflammation, immunoregulation, survival, and proliferation, as well as of RelB and p52, which are involved in lymphogenesis and B cell maturation (16). Cytosolic, inactive NF-κB is activated by the serine/threonine kinase IκB-kinase IKK (reviewed in ref. 17), a heterotrimer composed of the IKKα and IKKβ kinases and the regulatory IKKγ subunit. IKK phosphorylates the NF-κB inhibitor IκB-α, which leads to its dissociation from the transcription factor and generates a high-affinity binding site on IκB-α for the ubiquitin ligase β-TrCP, causing its subsequent ubiquitination and proteasomal degradation. Simultaneously, the dissociation of IκB-α unmasks a nuclear localization signal on NF-κB and renders it competent for translocation to the nucleus and DNA binding.

A pivotal role for activation of the NF-κB pathway in tumors as well as for survival of several tumor cell lines has been shown and can be correlated with tumor stages and outcome. Constitutively active NF-κB can be found, for example, in later-stage hormone-independent (estrogen receptor negative) breast cancer cell lines, but is absent from the earlier-stage hormone-dependent lines, such as MCF-7 and T47D (18). Furthermore, NF-κB is constitutively active in certain colorectal cancer cell lines, and 8 of 10 colorectal tumors tested showed enhanced NF-κB DNA binding activity when compared with adjacent normal mucosa (19). In addition, NF-κB is regarded as a therapeutic target in multiple myeloma (20) and Hodgkin's lymphoma (21).

**Note:** Supplementary data for this article are available at Cancer Research Online (http://cancerres.aacrjournals.org).

**Requests for reprints:** Markus Boehm, ALTANA Pharma AG, RDR/P3, Byk-Gulden-Str. 2, D-78467 Konstanz, Germany. Phone: 49-7531-844-537; Fax: 49-7531-849-4537; E-mail: markus.boehm@altanapharma.com.



doi:10.1158/0008-5472.CAN-05-4225

Even though smoking has been shown to induce NF-κB activation (22, 23), which can lead to asthma and other inflammatory processes, such as chronic obstructive pulmonary disease (24), surprisingly little is known about the prevalence of the NF-κB pathway in securing survival or inducing chemoresistance in lung tumors or lung cancer cell lines. One of the goals of this study, therefore, was the elucidation of the NF-κB activation status in human non–small cell lung cancer (NSCLC) cell lines. Moreover, we investigated the influence of HDI on the inducibility of the NF-κB pathway in NSCLC as well as their *in vivo* antitumor effects against NSCLC xenografts.

## Materials and Methods

**Cell culture and chemicals.** All cell lines were obtained from American Type Culture Collection (Wesel, Germany) and cultured in the recommended medium. Trichostatin A (TSA) was purchased from Sigma-Aldrich (Taufkirchen, Germany) and SAHA was synthesized in-house. Tumor necrosis factor-α (TNF-α) and interferon-α (IFN-α) were from Tebu-Bio (Offenbach, Germany).

**Electrophoretic mobility shift assay.** Cells were incubated with HDI for 24 hours before stimulation with 25 ng/mL of TNF-α for 30 minutes. Nuclear extracts were prepared according to the protocol of Active Motif (Rixensart, Belgium). Briefly, cells were washed with PBS, scraped off in PBS, centrifuged, resuspended in hypotonic buffer [20 mmol/L HEPES (pH 7.5), 5 mmol/L NaF, 10 μmol/L $Na_2MoO_4$, 0.1 mmol/L EDTA], and kept on ice for 15 minutes. NP40 was added to a final concentration of 0.5% and the suspension was recentrifuged. The pellet was resuspended in 20 mmol/L HEPES, 400 mmol/L NaCl, 0.1 mmol/L EDTA, 10 mmol/L NaF, 10 μmol/L $Na_2MoO_4$, 20% glycerol, 10 mmol/L β-glycerophosphate, 1 mmol/L DTT containing a cocktail of protease and phosphatase inhibitors (Sigma-Aldrich) and rocked on ice for 30 minutes. Then, the suspension was centrifuged for 10 minutes at 14,000 × *g*, 4°C and the supernatant was stored at −80°C.

Electrophoretic mobility shift assays (EMSA) were done using a double-stranded oligonucleotide (Invitrogen, Karlsruhe, Germany) containing a consensus κB binding site (5′-AGTTGAGGGGACTTTCCAGGC-3′—consensus κB region underlined). The oligonucleotide was end-labeled with [γ-$^{32}$P]ATP using T4 polynucleotide kinase (Amersham, Freiburg, Germany) and purified using MicroSpin G50 columns (Amersham). Nuclear extracts were incubated with 40 mmol/L HEPES/NaOH (pH 7.9), 120 mmol/L KCl, 8% Ficoll, 2 mmol/L DTT, 0.1 μg/μL poly(deoxyinosinic-deoxycytidylic acid), 0.1 μg/mL BSA at room temperature for 15 minutes. For supershift experiments, the nuclear extracts were preincubated with 4 μg of anti-p65 antibody (Santa Cruz Biotechnology, Heidelberg, Germany). The reaction mixture was subjected to electrophoresis in a 5% polyacrylamide gel. Gels were dried under vacuum and visualized with a FUJIFILM FLA-5000 Phosphorimager (Fuji Photo Film, Düsseldorf, Germany).

**Gene expression analysis.** After incubation with HDI for 24 hours and TNF-α stimulation for 4 hours, cells were washed with PBS, and total RNA was isolated using the RNeasy Mini Kit (Qiagen, Hilden, Germany). cDNA synthesis was carried out using reverse transcriptase from Roche Applied Science (Mannheim, Germany). Real-time PCR was employed to quantify human IκB-α, IL-8, c-Flip, Bcl-$x_L$, VEGF-c, TNF-α receptor-1 (TNFR1), and TRAIL receptor 2 (TRAIL-R2) transcripts and 18S rRNA (Applied Biosystems, Foster City, CA) from cDNA samples. All samples were analyzed in triplicate and probes were standardized with respect to total RNA and 18S-RNA. Results from three independent experiments were analyzed for statistical significance performing ANOVA with Dunnett's multiple comparison test using GraphPad Prism 4.0 software.

**Fluorescence flow cytometry.** A549 cells were either treated with HDI for 24 hours or left untreated. Cells were rinsed with PBS, detached with 0.2% EDTA/PBS solution at 37°C for 10 to 20 minutes, washed with PBS, and incubated with mouse $IgG_{2b}$ anti-human TNFR1 (Santa Cruz Biotechnology) monoclonal antibody for 30 minutes on ice. Thereafter, cells were washed with PBS and incubated with rabbit anti-mouse IgG antibody labeled with FITC (Calbiochem/Merck Biosciences, Schwalbach, Germany). After 30 minutes, cells were washed twice with PBS, resuspended in 1% formaldehyde/PBS, and analyzed using a FACS-Canto instrument (Becton Dickinson, Heidelberg, Germany). Data were analyzed employing FlowJo Software (TreeStar, Ashland, OR).

**Immunoblotting.** HDI and TNF-α treated cells were washed with PBS and lysed using 120 mmol/L NaCl, 50 mmol/L Tris/HCl (pH 7.4), 20 mmol/L NaF, 1% Triton X-100, 0.5% Na-desoxycholate, 0.1% SDS, 1 mmol/L $Na_3VO_4$, and protease inhibitor cocktail (Roche Applied Science). Lysates were subjected to SDS-PAGE, transferred to polyvinylidene difluoride membrane (Bio-Rad, Munich, Germany), and immunoblotted with anti-IκB-α, anti-phospho-IκB-α, anti-p-IKKα/IKKβ $Ser^{176/180}$ antibodies from Cell Signaling (Beverly, MA), anti-IKKα and anti-IKKβ antibodies from Biomol (Hamburg, Germany), anti-IKKγ and TNFR1 from Santa Cruz Biotechnology and anti-β-actin from Sigma-Aldrich, respectively. The membranes were washed with TBS containing 0.05% Tween 20 (Sigma-Aldrich) and incubated with secondary antibodies (Bio-Rad) conjugated with horseradish peroxidase. Protein bands were detected by chemiluminescence using the Lumi-Light$^{PLUS}$ Western blotting kit (Roche Applied Science).

**Nuclear translocation assay.** Cells were incubated with HDI for 24 hours. After stimulation with either 25 ng/mL TNF-α or 100 ng/mL IFN-α, cells were fixed with 3.7% formaldehyde at room temperature, washed with blocking buffer (0.3% Tween 20, 1% BSA in PBS), and permeabilized using 30 mmol/L NaCl, 0.54 mmol/L $Na_2HPO_4$, 0.3 mmol/L $KH_2PO_4$, 0.1% Triton X-100. Cells were washed in blocking buffer and incubated in blocking buffer containing anti-p65 antibody (Santa Cruz Biotechnology) for TNF-α or anti-STAT1 antibody (Santa Cruz Biotechnology) for IFN-α-stimulated cells for 1 hour. After washing with blocking buffer twice, Alexa-Fluor 488–labeled anti-mouse IgG or anti-rabbit IgG (Invitrogen) was added together with Hoechst 33342 dye (Molecular Probes/Invitrogen) for 1 hour. After washing thrice, the plates were scanned using the ArrayScan II high-content scan reader (Cellomics, Berkshire, United Kingdom).

**Xenograft study.** Female athymic NMRI *nu/nu* mice were inoculated s.c. into both flanks with 1 × $10^6$ A549 cells suspended in 500 μL PBS. The treatment groups consisted of 10 animals each. The treatment was given p.o. once a day after 21 days of growth, when tumors reached a volume of 100 $mm^3$. SAHA was prepared in a vehicle of 20% PEG 400 and 4% Methocel in $H_2O$. The tumor size was determined by externally measuring the tumors in two dimensions using a caliper. Volume ($V$) was calculated according to $V = (L \times W^2) \times 0.5$, where $L$ is length and $W$ is width of the tumor.

## Results

**NF-κB is inducible in NSCLC cell lines.** We first evaluated the NF-κB activation status in the two NSCLC model cell lines A549 and NCI-H460. To this end, we did EMSA experiments (Fig. 1*A*). In the absence of TNF-α, both cell lines showed only marginal binding of the NF-κB protein to the κB sites from the HIV-1 long terminal repeat (Fig. 1*A, lanes 1* and *3*). However, the NF-κB DNA binding capability could be enhanced significantly upon stimulation with TNF-α, indicating that both cell lines possess an inducible and functional NF-κB pathway (Fig. 1*A, lanes 2* and *4*). As a positive control for a cell line with constitutive activation of the NF-κB signaling pathway, we used Hodgkin's lymphoma HDLM-2 cells (25). There, strong NF-κB DNA binding was prevalent even in the absence of TNF-α and the NF-κB DNA binding efficiency could not be enhanced by the addition of TNF-α (Fig. 1*A, lanes 5* and *6*).

In order to test whether this inducibility of NF-κB DNA binding translated into changes in NF-κB target gene expression, we quantified IL-8 and IκB-α expression. As predicted from the EMSA

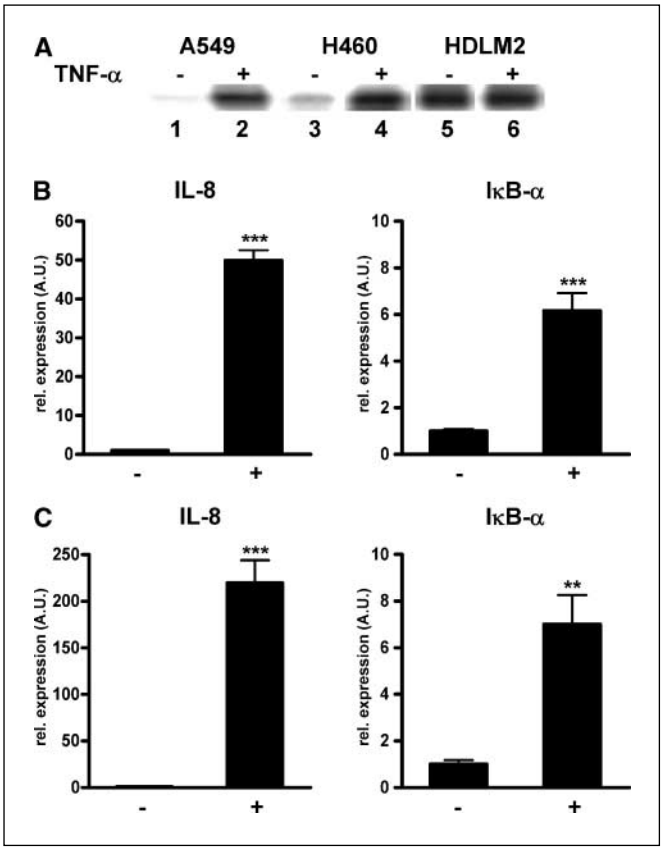


**Figure 1.** The NF-κB pathway is inducible in NSCLC cell lines. EMSA (*A*) and quantitative PCR (*B* and *C*) were used to study the status of NF-κB activation in human NSCLC cell lines. *A,* whole cell extracts from untreated as well as TNF-α (25 ng/mL; 30 minutes)–stimulated A549 and H460 NSCLC as well as HDLM2 Hodgkin's lymphoma cell lines were used to detect binding of NF-κB to κB binding sites. Total RNA, isolated from either untreated or TNF-α (25 ng/mL, 4 hours)–stimulated H460 (*B*) or A549 (*C*) cells, was used to quantify the relative expression of the NF-κB target genes IL-8 and IκB-α. **, $P < 0.01$; ***, $P < 0.001$, statistical significance was evaluated using an unpaired *t* test.

read-outs, we observed strong stimulation of gene expression for each of these target genes upon TNF-α treatment, thus indicating functional inducibility of the NF-κB pathway in NSCLC (Fig. 1*B* and *C*). Because information correlating HDAC inhibition with NF-κB signaling in NSCLC is sparse, we next sought to test the effect of HDI on the inducibility of the pathway.

**HDIs suppress TNFR1 expression and surface exposure in NSCLC.** Activation of NF-κB by TNF-α in noninflammatory cells, such as NSCLC tumor cells, requires binding to TNFR1 (26, 27). Thus, we decided to start by characterizing the effect of HDIs on TNFR1 gene expression in a panel of NSCLC cell lines from all three NSCLC subtypes. Treatment of eight cell lines for 24 hours with either SAHA or TSA caused reduction of TNFR1 gene expression to ~10% to 40% of control levels irrespective of the NSCLC subtype as measured by TaqMan PCR (Table 1). A more detailed analysis in NCI-H460 and A549 cells showed that increasing concentrations of each of the drugs led to a statistically significant, dose-dependent decrease in the TNFR1 message (Fig. 2*A, lanes 2-4, 5-7, 9-11*, and *12-14*) and also caused reduced TNFR1 protein levels (Fig. 2*B, lanes 2-4* and *5-7*), when compared with control cells (Fig. 2*A, lanes 1* and *8*; Fig. 2*B, lane 1*). As an internal control for the specificity and relevance of the observed TNFR1 down-regulation, we measured the expression of TRAIL-R2. Expression of this cell surface molecule has been previously shown to increase upon HDI treatment (28–30), which results in synergistic apoptosis induction of TRAIL and HDIs, such as SAHA, sodium butyrate (NaB), and TSA (31). Indeed, at concentrations in which TNFR1 expression was suppressed, TRAIL-R2 expression was increased (Fig. 2*C, lanes 2-4, 5-7, 9-11*, and *12-14*). If functionally important, the strong down-regulation of TNFR1 mRNA and protein should also result in reduced surface exposure of the receptor. To obtain evidence for this, we probed for surface TNFR1 using FACS measurements. In line with the findings for TNFR1 message and protein levels, we found that increasing concentrations of SAHA (Fig. 2*D, b-d*) and TSA (Fig. 2*D, f-h*) reduced the surface exposure of TNFR1: upon the addition of SAHA or TSA, the main fluorescence intensity shifted from $10^4$ as observed in untreated cells (Fig. 2*D, a*) towards $10^3$, the value also seen for the isotype control sample (Fig. 2*D, e*).

Thus, in summary, both HDIs caused a drastic reduction of TNFR1 gene expression in a number of NSCLC cell lines, resulting in lowered TNFR1 protein levels and exposure on the cell surface as shown for NCI-H460 and A549. In order to elucidate whether this finding would bear functional consequences for the inducibility of the NF-κB pathway, we decided to characterize several components along the pathway for their response to combined HDI and TNF-α treatment, and to ultimately test for the influence of HDI incubation on TNF-α-stimulated NF-κB target gene expression.

**IKK phosphorylation is influenced by treatment with HDIs resulting in reduced inhibitor phosphorylation and degradation.** Upon the binding of TNF-α to TNFR1, a signaling cascade involving RIP-1 and TRAF proteins, which form a complex with the TNFR1 cytosolic domain, induces IKK recruitment and activation. This results in phosphorylation of IKK on serines 176/180 and 177/181 of the α and β subunits, respectively. Several kinases have been described to carry out this phosphorylation, among which, NIK possesses a certain preference for IKKα (32), whereas MEKK3 is more specific for IKKβ (33). TNFR1 down-regulation should decrease the potential of TNF-α to induce IKK phosphorylation. Accordingly, we found reduced levels of phosphorylated IKKα/IKKβ 10 minutes after the addition of TNF-α in cells preincubated with HDIs (Fig. 3*A, lanes 1-3* and *5-7*) when compared with cells without HDIs (Fig. 3*A, lanes 4* and *8*). IKK protein levels, on the other hand, seemed to be unaffected. Figure 3*B* shows that in NCI-H460 as well as in A549, the intracellular amounts of all three subunits of IKK—IKKα, IKKβ, and IKKγ—were unchanged after 24 hours of incubation with HDIs.

We then tested whether the lack of activating phosphorylation on IKK would translate into altered phosphorylation and degradation of the inhibitor IκB-α. In line with the previous findings, immunoblotting experiments revealed that in SAHA-treated and TSA-treated NSCLC cells, IκB-α phosphorylation was largely undetectable after 4 minutes of TNF-α stimulation (Fig. 3*C, upper panel, lanes 1-3* and *5-7*), whereas control cells showed appreciable phosphorylation of IκB-α (Fig. 3*C, upper panel, lanes 4* and *8*). This phosphorylation defect resulted in stabilization of the inhibitor. In NCI-H460 and in A549, 10 minutes after the addition of TNF-α, IκB-α was undetectable in control cells (Fig. 3*C, lower panel, lanes 4* and *8*), whereas the respective protein band was present under increasing concentrations of SAHA (Fig. 3*C, lower panel, lanes 1-3*) as well as TSA (Fig. 3*C, lower panel, lanes 5-7*).

**Table 1.** HDIs cause down-regulation of TNFR1 mRNA in a variety of human NSCLC cell lines

| Cell line | NSCLC subtype | Relative expression of TNFR1 (% of untreated control ± SD) | | | |
|---|---|---|---|---|---|
| | | 10 μmol/L SAHA | 50 μmol/L SAHA | 2 μmol/L TSA | 4 μmol/L TSA |
| A-427 | Adenocarcinoma | 36 ± 6 | 21 ± 1 | 20 ± 3 | 25 ± 2 |
| A549 | Adenocarcinoma | 29 ± 4 | 13 ± 2 | 12 ± 1 | 12 ± 2 |
| NCI-H23 | Adenocarcinoma | 21 ± 1 | 7 ± 1 | 6 ± 1 | 7 ± 1 |
| NCI-H1563 | Adenocarcinoma | 91 ± 5 | 29 ± 3 | 21 ± 2 | 26 ± 2 |
| NCI-H1703 | Adenocarcinoma | 35 ± 1 | 15 ± 2 | 18 ± 2 | 17 ± 1 |
| NCI-H460 | Large cell carcinoma | 24 ± 1 | 9 ± 1 | 6 ± 1 | 6 ± 1 |
| NCI-H520 | Squamous cell carcinoma | 23 ± 1 | 9 ± 1 | 8 ± 0 | 7 ± 0 |
| NCI-H2170 | Squamous cell carcinoma | 40 ± 2 | 10 ± 1 | 10 ± 1 | 9 ± 1 |

NOTE: NSCLC cell lines were treated with HDIs for 24 hours and expression of TNFR1 was assayed by TaqMan PCR.

**HDIs inhibit nuclear translocation of NF-κB.** In order to bind to the promoter regions in its target genes, NF-κB needs to first translocate from the cytosol into the nucleus. Given the altered inhibitor degradation, we asked whether incubation with HDIs would consequently influence NF-κB nuclear translocation upon TNF-α stimulation. To this end, we employed Array Scan–based translocation measurements, which quantify the cytosolic and nuclear fractions of NF-κB. Indeed, at concentrations in which TNFR1 was down-regulated, HDIs led to a reduction of nuclear NF-κB (Fig. 4*A* and *B*). When compared with control cells without HDIs, NF-κB translocation kinetics differed profoundly in two aspects: first, a lag phase of several (up to 10) minutes for onset of nuclear translocation was observed. Secondly, the overall level of translocated NF-κB remained much lower in HDI-treated cells than in control cells. This effect became dominant after 15 minutes, when HDI-treated cells leveled out the amount of nuclear NF-κB at ~50% of untreated control cells. Thus, the nuclear translocation studies suggested that the pool of cytosolic NF-κB was not only activated more slowly, but that it also had a lower nuclear translocation potential once it became activated. To determine whether this translocation defect was specific for the NF-κB pathway or might be a matter of general nuclear import down-regulation, we compared the TNF-α-induced translocation of NF-κB with the IFN-α-induced translocation of STAT1 (Fig. 4*C* and *D*). We found that SAHA, in a dose-dependent manner, reduced only the TNF-α-stimulated translocation of NF-κB (Fig. 4*C*). No inhibitory effect was observed for the IFN-α-induced nuclear shuttling of STAT1 (Fig. 4*D*), thus indicating that HDIs specifically block NF-κB's nuclear import.

**NF-κB DNA binding and target gene expression are decreased by HDIs.** Thus far, we were able to show that the HDI-mediated effects on TNFR1 also caused defective IKK and IκB-α phosphorylation, and reduced NF-κB nuclear translocation upon addition of TNF-α. In order to fully establish the proof of concept though, we wanted to determine whether the above-described effects would also translate into alterations of NF-κB DNA binding and of NF-κB-mediated target gene expression.

We employed EMSA measurements to assay for the inducibility of NF-κB DNA binding after 24 hours of incubation with HDIs (Fig. 5). Increasing concentrations of SAHA (Fig. 5*A, lanes 3-5*) and TSA (Fig. 5*A, lanes 6-8*) lowered the amount of NF-κB bound to DNA below the level seen in stimulated cells (Fig. 5*A, lane 2*). Furthermore, the supershift experiment shown in Fig. 5*B* established the identity of the shifted band as p65-containing NF-κB. The addition of an anti-p65 antibody led to increased retardation of the respective band (Fig. 5*B, lanes 1 and 2*). Moreover, Fig. 5*B* (*lanes 2, 4*, and *6*) shows the decrease in p65 upon incubation with SAHA or TSA (see arrows).

The reduced signal in the EMSA experiments coincided with a repression of TNF-α-induced NF-κB-dependent gene expression (Fig. 5*C*). Relative expression levels of IκB-α (*top*), c-Flip (*second*), Bcl-$x_L$ (*third*), and VEGF-c (*bottom*) were decreased at concentrations of SAHA and TSA in which NF-κB DNA binding was reduced and TNFR1 was down-regulated.

In conclusion, these results show that HDIs cause TNFR1 down-regulation, which triggers desensitization of the NF-κB pathway, and ultimately results in reduced induction of NF-κB target gene expression after the addition of TNF-α.

**SAHA inhibits growth of A549 xenografts.** In order to determine whether these findings would bear any significance for the treatment of NSCLC, we evaluated the *in vivo* antitumor effect of SAHA in athymic nude mice carrying A549 tumor xenografts obtained 21 days after s.c. inoculation of $1 \times 10^6$ cells into both flanks of the animals. As shown in Fig. 6, oral treatment with 120 mg/kg SAHA led to growth retardation of the tumor compared with the placebo-treated group. Whereas the tumors of the placebo group reached a final mean tumor volume of ~700 $mm^3$, tumors of the SAHA-treated group grew to a mean volume of only 460 $mm^3$. The tumor/control ratio in this model was 0.5, revealing that SAHA inhibited tumor growth by 50%.

## Discussion

HDIs have recently garnered great interest in the oncology community (2, 5, 34). Their possible therapeutic use holds great promise for the treatment of hematologic as well as solid tumors. Nevertheless, their mechanism of action is still unresolved with manifold observations ranging from the activation of gene expression by the alleviation of epigenetic blocks, such as histone deacetylation and methylation, to the modification (i.e.,

acetylation) of other important cellular proteins, such as tubulin (35, 36), p53 (37, 38), or Hsp90 (39), themselves regulators of many important intracellular pathways in a variety of cellular systems.

To explore which, if any, of the hitherto described mechanisms would apply to the molecular layout in NSCLC, we measured the effect of two hydroxamate-type HDIs on several human NSCLC cell lines and uncovered a yet undescribed reduction in the

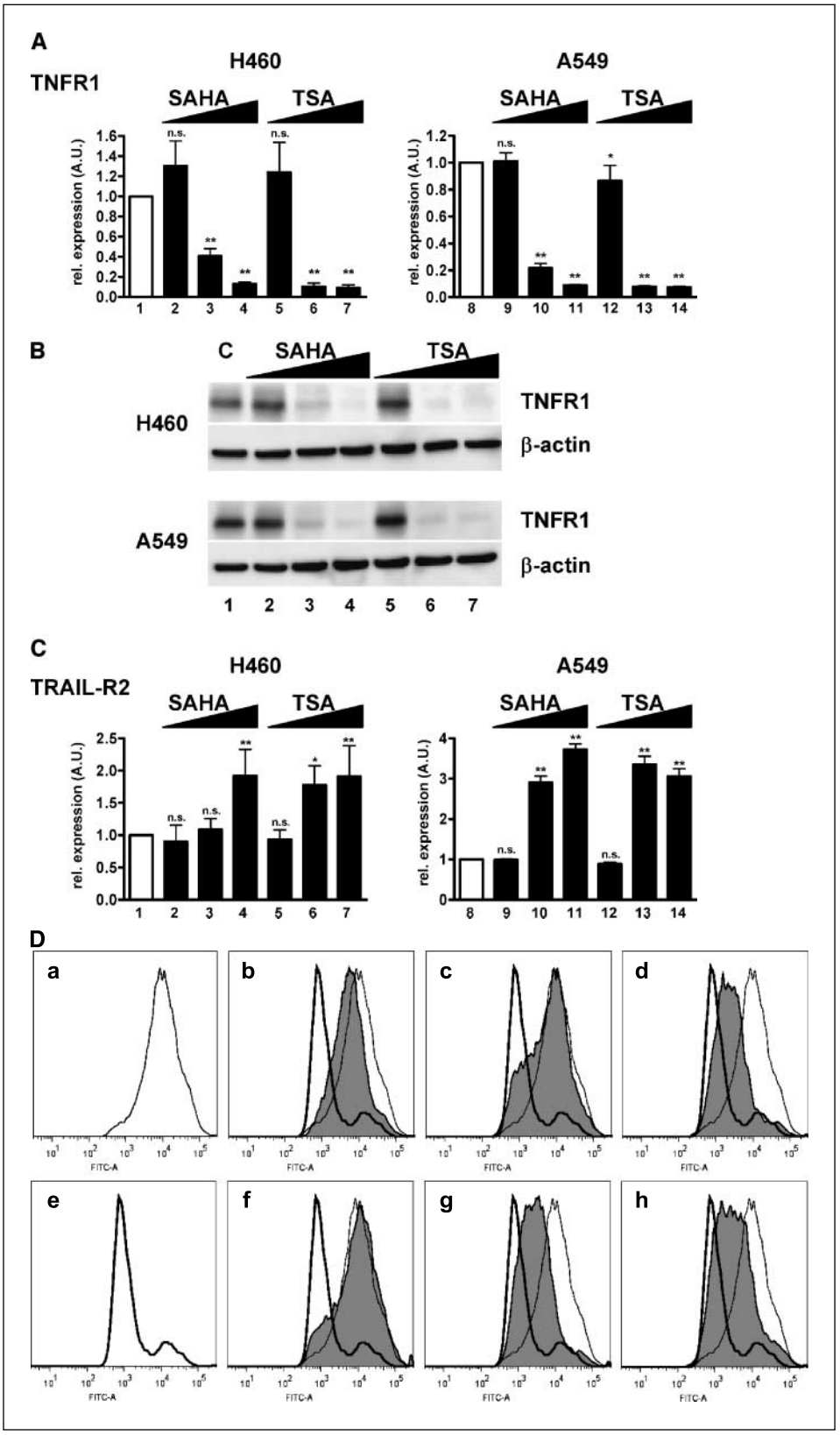


**Figure 2.** HDIs down-regulate TNFR1 mRNA and protein, and decrease receptor exposure at the cell surface. H460 and A549 cells were treated with various concentrations of HDIs for 24 hours and assayed for RNA and protein expression. Total RNA was used to quantify the relative expression of (*A*) TNFR1 and (*C*) TRAIL-R2: *lanes 1* and *8,* no HDI; *lanes 2-4* and *9-11,* 1 μmol/L, 10 μmol/L, and 50 μmol/L SAHA; *lanes 5-7,* and *12-14,* 200 nmol/L, 2 μmol/L, 4 μmol/L TSA. Columns, mean of three independent experiments; bars, ±SD. Statistical significance was evaluated using ANOVA with Dunnett's multiple comparison test (n.s., not statistically significant; *, $P < 0.05$; **, $P < 0.01$). *B,* H460 and A549 cells were preincubated with various concentrations of HDIs for 24 hours, lysed and immunoblotted for TNFR1: *lane 1,* no HDI; *lanes 2-4,* 1 μmol/L, 10 μmol/L, and 50 μmol/L SAHA; *lanes 5-7,* 200 nmol/L, 2 μmol/L, and 4 μmol/L TSA; loading control, β-actin. *D,* A549 cells were treated with SAHA or TSA for 24 hours, detached and reacted with mouse monoclonal antibody against TNFR1 and FITC conjugated anti-mouse antibody and analyzed on a BD FACS-Canto. *a,* no HDI; *b-d,* 1 μmol/L, 10 μmol/L, and 50 μmol/L SAHA; *e,* isotype control; *f-h,* 200 nmol/L, 2 μmol/L, 4 μmol/L TSA. Thin and thick lines in (*b-d*) and (*f-h*) indicate the position of the medium and isotype controls, respectively.

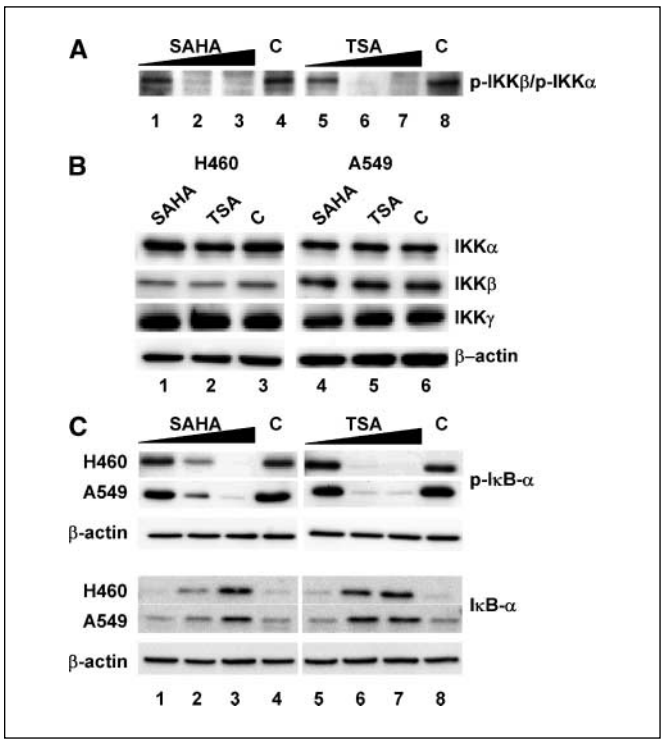


**Figure 3.** Incubation with HDIs changes IKK activation and reduces IκB-α phosphorylation and degradation, but does not alter IKK protein levels. A549 and H460 cells were preincubated with HDIs for 24 hours and stimulated with TNF-α for 4 minutes (p-IκB-α) or 10 minutes (all others). Cell lysates were immunoblotted for (*A*) p-IKKα/β, (*B*) IKKα, IKKβ or IKKγ, as well as (*C*) p-IκB-α or IκB-α protein levels. *A,C, lanes 1-3*, 1 μmol/L, 10 μmol/L, 50 μmol/L SAHA; *lanes 4* and *8*, no HDI; *lanes 5-7,* 200 nmol/L, 2 μmol/L, 4 μmol/L TSA. *B, lanes 1* and *4*, 50 μmol/L SAHA; *lanes 2* and *5,* 4 μmol/L TSA; *lanes 3 and 6,* no HDI. Loading control: β-actin.

expression of TNFR1. We did a thorough analysis of the influence of HDIs on the well-defined NSCLC cell lines, A549 and NCI-H460, in which TNFR1 is the only TNF-α receptor present (26, 27). Accordingly, the reduction in TNFR1 expression correlated with dramatic consequences for the inducibility of the NF-κB pathway: delayed IκB-α phosphorylation, retarded IκB-α degradation, a subsequent block in the translocation of NF-κB from the cytosol to the nucleus, and finally reduced NF-κB DNA binding and target gene expression. Interestingly, the reduced nuclear shuttling of NF-κB upon TNF-α stimulation after HDAC inhibition was previously noted in murine RAW264 macrophages (40), as well as in HT-29 colon cancer cells (41) after treatment with TSA and NaB, and TNF-α stimulation. We observed these effects in the NSCLC cell lines at concentrations in which cellular viability after 24 hours was slightly decreased to ~75% as judged by Alamar blue measurements. As internal control read-outs for the specificity of the effect of HDIs on the NF-κB pathway, we showed the literature-described up-regulation of TRAIL-R2 (34–36), which occurred in the same HDI concentration range, lack of an effect on IFN-α signaling, and unaltered levels of intracellular proteins such as IKK and β-actin.

It is important to point out that the findings presented here are in contrast with two studies from one laboratory, describing the activation of NF-κB signaling by HDIs in NSCLC (42, 43). There, HDIs were postulated to activate NF-κB target gene expression, which was used to argue for the synergy between inhibitors of HDACs and NF-κB for NSCLC tumor treatment. Both reports focused on differences in the expression of a 3x-κB-luciferase construct and of the NF-κB target gene IL-8. Curiously though, upon incubation with HDIs, no degradation of the inhibitor IκB-α or NF-κB DNA binding could be shown (43), both hallmarks of NF-κB signaling. When we investigated the influence of HDIs on NF-κB target gene expression, we confirmed the reported ~5-fold activation of IL-8 gene expression in A549 (data not shown) but observed that the addition of TNF-α, a well-described NF-κB activator, caused an ~200-fold activation of IL-8 gene expression (see Fig. 1*C*), and that under these conditions, the addition of HDI became inhibitory to the activation of NF-κB. Moreover, we found that expression of the IκB-α gene, a highly specific read-out for NF-κB activation, was not increased by the addition of HDIs alone and was only induced in TNF-α-treated samples. Taken together, these observations and the lack of NF-κB activation–specific read-outs upon HDI incubation reported by Mayo et al. (43), suggest that the previously noted activation of NF-κB by HDI was weak in magnitude and possibly nonspecific.

Several recent publications report on the influence of HDI treatment on the NF-κB activation status in model systems other than NSCLC. Among them, the most comprehensive was a measurement of the release of cytokines in BALB/c mice treated with lipopolysaccharide. There, except for IL-1β precursor, IL-1 receptor antagonist, and IL-8, SAHA treatment had an inhibitory quality, arguing for an NF-κB inhibitory effect of HDIs (44). Besides this, literature describing the effects of HDIs on tumor cells is conflicting with respect to the observed phenotype and its consequences (reviewed in refs. 45, 46), which can be illustrated regarding the question of NF-κB acetylation. Even though this seems to be a focused, relatively straightforward, and accessible read-out, the question of whether p65 is itself acetylated and, if so, which functional consequences arise thereof, is a matter of debate. Several reports indicate that HDIs regulate NF-κB activity by acetylation of the p65 subunit (11, 12, 45, 47, 48). Direct acetylation of the NF-κB subunit p65 in 293T cells that was enhanced by treatment with TSA was first described by Chen and colleagues (11). The authors claim reduced binding of the inhibitor IκB-α to NF-κB after treatment with TSA, and thus enhanced TNF-α-induced gene expression of a luciferase reporter construct. Later, Kiernan et al. showed that in Jurkat cells, TSA enhanced PMA-mediated acetylation of p65 (12), which negatively influenced the DNA-binding capability of p65, and was thus speculated to pose a negative feedback mechanism. Adam et al., on the other hand, were unable to show acetylation of p65 (49), but showed the activation of NF-κB signaling by HDIs resulting from a persistent activation of IKK in HeLa cells. Similarly to this latter report, in our experiments, several attempts to detect acetylated p65 in samples from HDI-treated cells either from whole cell lysates or from immunoprecipitated p65 and by using several acetyl lysine–specific antibodies, failed (data not shown). However, given the observed cytosolic retention of NF-κB, we find this not surprising. The methyltransferase activities p300/CBP and PCAF as well as the deacetylase enzymes HDAC1 and HDAC3 involved in the proposed acetylation/deacetylation reaction of NF-κB are nuclear activities. Accordingly, Benkirane and colleagues describe that NF-κB stimulation is required for acetylation of p65 in the nucleus (12). This acetylation is then enhanced in the presence of TSA. No p65 acetylation is observed, however, by incubation

with TSA alone. Thus, p65 acetylation/deacetylation is thought to be a strictly nuclear event (reviewed in ref. 45). In the NSCLC cell lines used here, HDIs inhibited the activation of NF-κB far upstream of its nuclear translocation. Thus, a likely explanation for the absence of detectable levels of acetylated p65 in this setting is that the cytosolically retarded transcription factor is prevented from acetylation by not entering the nucleus in the first place. Possibly, in cellular systems with constitutively active NF-κB that frequently travels the nucleus, acetylation of p65 is a major regulatory event, but it does not seem to be under the conditions of inducibly active NF-κB signaling in NSCLC.

The heterogeneity of the results presented in the literature, that are in part contradictory, stresses the need for careful definition of the NF-κB activation status in the cellular system used and the characterization of the HDI-mediated alterations in a pathway of interest using as many experimentally accessible read-outs as possible. Being first and foremost regulators of gene expression, HDIs have a multitude of effects, and thus, in order to separate specific from unspecific effects, coherence of many experimental findings is invaluable for correctly interpreting the results.

In our own Array Scan experiments, we noted that at later time points, a significant amount of NF-κB was able to translocate into the nucleus in HDI-treated, TNF-α-stimulated cells without causing obvious consequences for NF-κB DNA binding as well as NF-κB target gene expression. As, according to the current paradigm, nuclear translocation requires inhibitor degradation, we assayed for IκB-α phosphorylation and degradation dynamics at these later time points. Surprisingly, given the low abundance of TNFR1 on the cell surface and the lack of target gene expression, we found that phosphorylated IκB-α and overall IκB-α in HDI-treated cells reached the levels of untreated control cells after 10 and 15 minutes of TNF-α treatment, respectively (Supplementary Fig. S1). This indicated a kinetic defect in IκB-α phosphorylation and degradation rather than an overall inhibition of IKK activity and perfectly fitted the observed NF-κB nuclear translocation dynamics: degradation of IκB-α reached the level of control cells ~15 minutes after the addition of TNF-α, and Array Scan measurements pointed to an increase in nuclear shuttling at exactly that time point. Obviously, the remaining few TNFR1 molecules at the cell surface allowed for some activation of IKK, IκB-α degradation, and subsequent NF-κB translocation. The fact

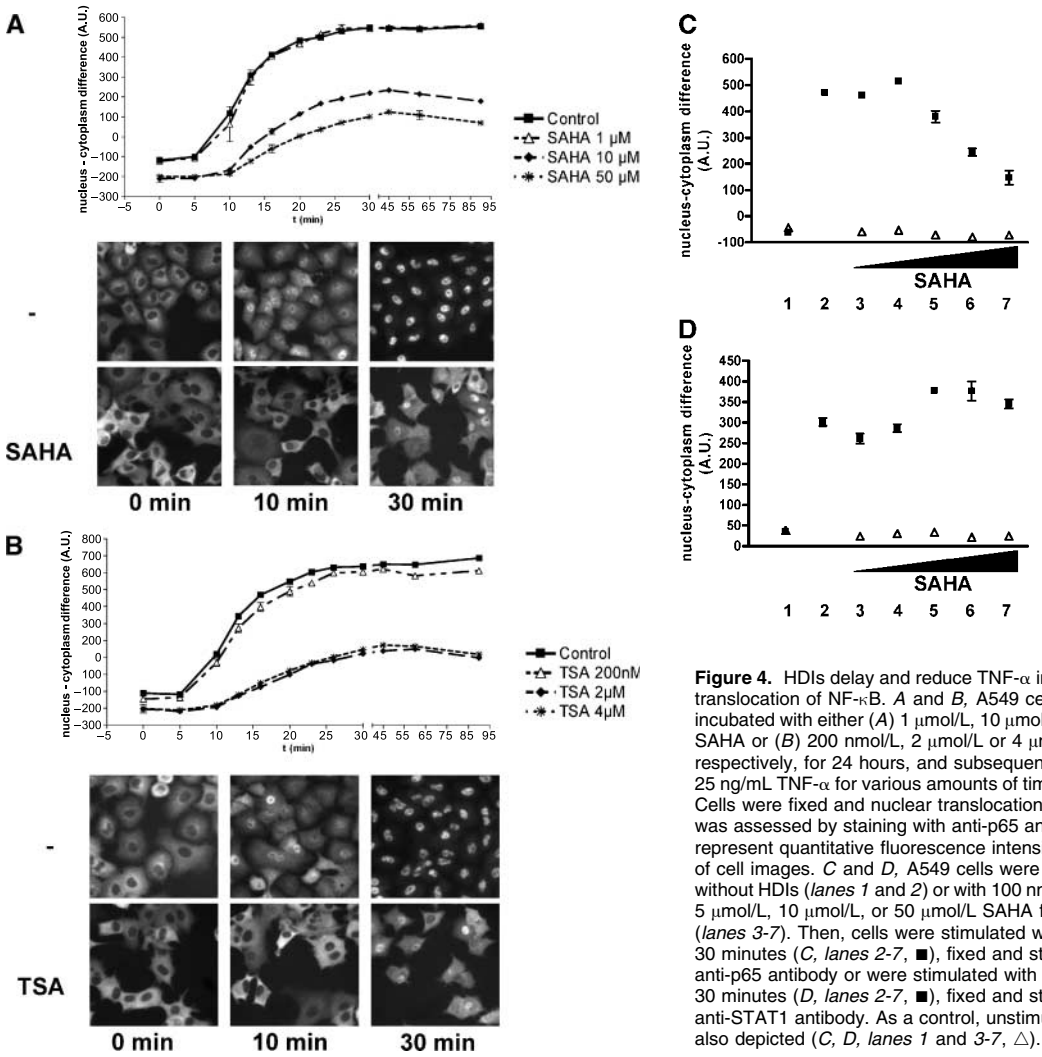


**Figure 4.** HDIs delay and reduce TNF-α induced nuclear translocation of NF-κB. *A* and *B,* A549 cells were incubated with either (*A*) 1 μmol/L, 10 μmol/L or 50 μmol/L SAHA or (*B*) 200 nmol/L, 2 μmol/L or 4 μmol/L TSA, respectively, for 24 hours, and subsequently treated with 25 ng/mL TNF-α for various amounts of time as indicated. Cells were fixed and nuclear translocation of NF-κB was assessed by staining with anti-p65 antibody. Graphs represent quantitative fluorescence intensity read-outs of cell images. *C* and *D,* A549 cells were incubated without HDIs (*lanes 1* and *2*) or with 100 nmol/L, 1 μmol/L, 5 μmol/L, 10 μmol/L, or 50 μmol/L SAHA for 24 hours (*lanes 3-7*). Then, cells were stimulated with TNF-α for 30 minutes (*C, lanes 2-7*, ■), fixed and stained with anti-p65 antibody or were stimulated with IFN-α for 30 minutes (*D, lanes 2-7*, ■), fixed and stained with anti-STAT1 antibody. As a control, unstimulated cells are also depicted (*C, D, lanes 1* and *3-7*, △).

that this delayed translocation of presumably inhibitor-free NF-κB would not result in NF-κB target gene expression suggests that only rapid and excessive translocation of NF-κB might possess sufficient transactivating potential to induce gene expression. Physiologically, this failsafe mechanism could guard against erroneous induction of target gene expression caused by leakage of NF-κB into the nucleus in unstimulated cells.

It is noteworthy that, in addition to the effects described above, during the 24-hour HDI incubation period in NCI-H460, but not in A549 cells, we observed a steady increase in expression of the NF-κB inhibitory subunit p100. This expression was both dose-dependent and time-dependent, whereas expression of p105, another inhibitory NF-κB subunit, decreased (data not shown). Coimmunoprecipitation experiments showed an HDI concentration–dependent increase in p100-p65 binding (data not shown), indicating that an increased protein concentration of p100 was sufficient to recruit an ever-higher amount of p65 into a translocation-deficient state. However, the lack of this observation in A549 along with the fact that short interfering RNA experiments targeting p100 in NCI-H460 revealed no influence on NF-κB inducibility (data not shown), led us to conclude that the p100 up-regulation in NCI-H460 could not explain the reduced NF-κB target gene expression caused by HDIs.

Somewhat contradictory to the effects observed at higher HDI concentrations, we noted that in one of the cell lines (NCI-H460), the lowest HDI concentration led to an apparent up-regulation of the TNFR1 message. This also translated into apparent increases of NF-κB target gene expression. In order to evaluate the significance of these observations, we applied statistical analysis to three independent replicates of the gene expression measurements. ANOVA followed by Dunnett's multiple comparison test revealed that the observed increases were not statistically significant for TNFR1 as well as for two of the four target genes. Yet, for c-Flip and VEGF-c, a statistically significant

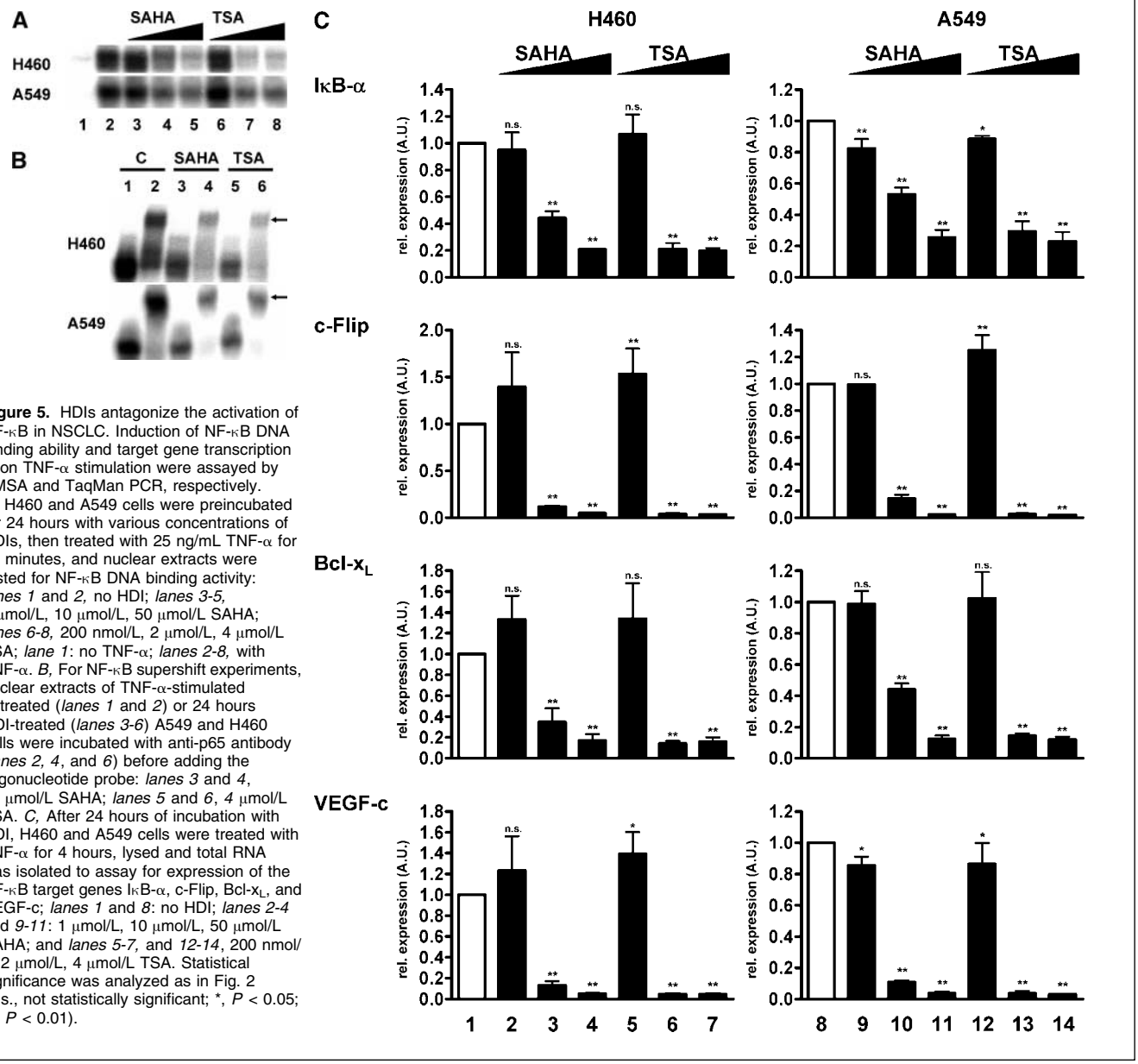


**Figure 5.** HDIs antagonize the activation of NF-κB in NSCLC. Induction of NF-κB DNA binding ability and target gene transcription upon TNF-α stimulation were assayed by EMSA and TaqMan PCR, respectively. *A,* H460 and A549 cells were preincubated for 24 hours with various concentrations of HDIs, then treated with 25 ng/mL TNF-α for 30 minutes, and nuclear extracts were tested for NF-κB DNA binding activity: *lanes 1* and *2,* no HDI; *lanes 3-5,* 1 μmol/L, 10 μmol/L, 50 μmol/L SAHA; *lanes 6-8,* 200 nmol/L, 2 μmol/L, 4 μmol/L TSA; *lane 1*: no TNF-α; *lanes 2-8,* with TNF-α. *B,* For NF-κB supershift experiments, nuclear extracts of TNF-α–stimulated untreated (*lanes 1* and *2*) or 24 hours HDI-treated (*lanes 3-6*) A549 and H460 cells were incubated with anti-p65 antibody (*lanes 2, 4*, and *6*) before adding the oligonucleotide probe: *lanes 3* and *4*, 50 μmol/L SAHA; *lanes 5* and *6*, *4* μmol/L TSA. *C,* After 24 hours of incubation with HDI, H460 and A549 cells were treated with TNF-α for 4 hours, lysed and total RNA was isolated to assay for expression of the NF-κB target genes IκB-α, c-Flip, Bcl-$x_L$, and VEGF-c; *lanes 1* and *8*: no HDI; *lanes 2-4* and *9-11*: 1 μmol/L, 10 μmol/L, 50 μmol/L SAHA; and *lanes 5-7,* and *12-14*, 200 nmol/L, 2 μmol/L, 4 μmol/L TSA. Statistical significance was analyzed as in Fig. 2 (n.s., not statistically significant; *, $P < 0.05$; **, $P < 0.01$).

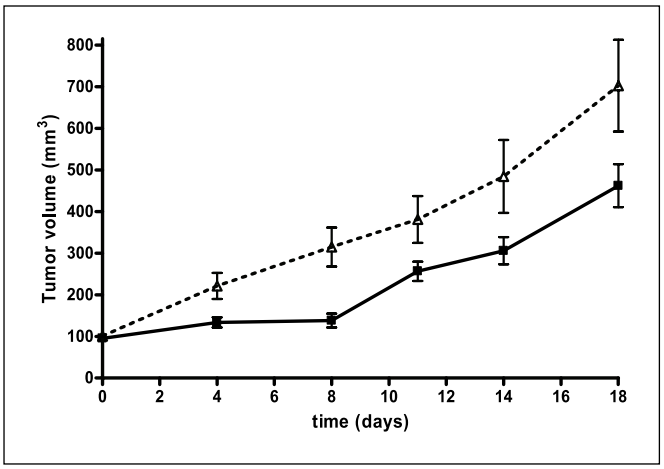


**Figure 6.** SAHA significantly reduces the growth of human A549 NSCLC xenografts *in vivo*. Twenty nude mice, each bearing two established A549 tumors were treated p.o. daily with either vehicle control (···△···, $n = 10$) or SAHA at a dose of 120 mg/kg (—■—, $n = 10$). Tumor growth is illustrated by mean tumor volume ± SE.

increase in mRNA upon TSA treatment could be found in NCI-H460. In summary, because the overall effect was very small and strictly limited to NCI-H460, we concluded that, in contrast to the excessive down-regulation at higher concentrations, this effect would most likely not be of general relevance for NSCLC if at all. Nevertheless, even though apparently not functionally important for NF-κB signaling in this context, this finding reiterates the fact that the inhibition of HDACs could create pleiotropic effects in different target cells which require extensive validation and a close correlation with a functional read-out in multiple cellular systems.

## Acknowledgments

Received 11/28/2005; revised 2/3/2006; accepted 3/21/2006.

The costs of publication of this article were defrayed in part by the payment of page charges. This article must therefore be hereby marked *advertisement* in accordance with 18 U.S.C. Section 1734 solely to indicate this fact.

We are indebted to M. Broemer (MDC, Berlin) and C. Scheidereit (MDC, Berlin) for providing Hodgkin's lymphoma cell lines, to H.P. Hofmann for help with TaqMan PCR, to M. Römmele for excellent assistance in evaluating the *in vivo* antitumor efficacy of SAHA, and to T. Heinzel (University of Jena), Karl Sanders and Thomas Maier for critical discussion and advice.

## References

1. Drummond DC, Noble CO, Kirpotin DB, Guo Z, Scott GK, Benz CC. Clinical development of histone deacetylase inhibitors as anticancer agents. Annu Rev Pharmacol Toxicol 2005;45:495–528.
2. Marks PA, Jiang X. Histone deacetylase inhibitors in programmed cell death and cancer therapy. Cell Cycle 2005;4:549–51.
3. La Thangue NB. Histone deacetylase inhibitors and cancer therapy. J Chemother 2004;16 Suppl 4:64–7.
4. Marks PA, Richon VM, Miller T, Kelly WK. Histone deacetylase inhibitors. Adv Cancer Res 2004;91:137–68.
5. Villar-Garea A, Esteller M. Histone deacetylase inhibitors: understanding a new wave of anticancer agents. Int J Cancer 2004;112:171–8.
6. Richon VM, Webb Y, Merger R, et al. Second generation hybrid polar compounds are potent inducers of transformed cell differentiation. Proc Natl Acad Sci U S A 1996;93:5705–8.
7. Joseph J, Mudduluru G, Antony S, Vashistha S, Ajitkumar P, Somasundaram K. Expression profiling of sodium butyrate (NaB)-treated cells: identification of regulation of genes related to cytokine signaling and cancer metastasis by NaB. Oncogene 2004;23:6304–15.
8. Wang S, Yan-Neale Y, Zeremski M, Cohen D. Transcription regulation by histone deacetylases. Novartis Found Symp 2004;259:238–45.
9. Mitsiades CS, Mitsiades NS, McMullan CJ, et al. Transcriptional signature of histone deacetylase inhibition in multiple myeloma: biological and clinical implications. Proc Natl Acad Sci U S A 2004;101:540–5.
10. Minucci S, Pelicci PG. Histone deacetylase inhibitors and the promise of epigenetic (and more) treatments for cancer. Nat Rev Cancer 2006;6:38–51.
11. Chen L, Fischle W, Verdin E, Greene WC. Duration of nuclear NF κB action regulated by reversible acetylation. Science 2001;293:1653–7.
12. Kiernan R, Bres V, Ng RW, et al. Post-activation turn-off of NF κB-dependent transcription is regulated by acetylation of p65. J Biol Chem 2003;278:2758–66.
13. Hu J, Colburn NH. Histone deacetylase inhibition down-regulates cyclin D1 transcription by inhibiting nuclear factor-κB/p65 DNA binding. Mol Cancer Res 2005;3:100–9.
14. Baldwin AS, Jr. Series introduction: the transcription factor NF-κB and human disease. J Clin Invest 2001;107:3–6.
15. Aggarwal BB. Nuclear factor-κB: the enemy within. Cancer Cell 2004;6:203–8.
16. Karin M, Yamamoto Y, Wang QM. The IKK NF-κB system: a treasure trove for drug development. Nat Rev Drug Discov 2004;3:17–26.
17. Bonizzi G, Karin M. The two NF-κB activation pathways and their role in innate and adaptive immunity. Trends Immunol 2004;25:280–8.
18. Nakshatri H, Bhat-Nakshatri P, Martin DA, Goulet RJ, Jr., Sledge GW, Jr. Constitutive activation of NF-κB during progression of breast cancer to hormone-independent growth. Mol Cell Biol 1997;17:3629–39.
19. Lind DS, Hochwald SN, Malaty J, et al. Nuclear factor-κB is upregulated in colorectal cancer. Surgery 2001;130:363–9.
20. Hideshima T, Chauhan D, Richardson P, et al. NF-κB as a therapeutic target in multiple myeloma. J Biol Chem 2002;277:16639–47.
21. Yung L, Linch D. Hodgkin's lymphoma. Lancet 2003;361:943–51.
22. Anto RJ, Mukhopadhyay A, Shishodia S, Gairola CG, Aggarwal BB. Cigarette smoke condensate activates nuclear transcription factor-κB through phosphorylation and degradation of IκB(α): correlation with induction of cyclooxygenase-2. Carcinogenesis 2002;23:1511–8.
23. Shen Y, Rattan V, Sultana C, Kalra VK. Cigarette smoke condensate-induced adhesion molecule expression and transendothelial migration of monocytes. Am J Physiol 1996;270:H1624–33.
24. Wright JG, Christman JW. The role of nuclear factor κB in the pathogenesis of pulmonary diseases: implications for therapy. Am J Respir Med 2003;2:211–9.
25. Krappmann D, Emmerich F, Kordes U, Scharschmidt E, Dorken B, Scheidereit C. Molecular mechanisms of constitutive NF-κB/Rel activation in Hodgkin/Reed-Sternberg cells. Oncogene 1999;18:943–53.
26. Shimomoto H, Hasegawa Y, Nozaki Y, et al. Expression of tumor necrosis factor receptors in human lung cancer cells and normal lung tissues. Am J Respir Cell Mol Biol 1995;13:271–8.
27. Nakamura H, Hino T, Kato S, Shibata Y, Takahashi H, Tomoike H. Tumour necrosis factor receptor gene expression and shedding in human whole lung tissue and pulmonary epithelium. Eur Respir J 1996;9:1643–7.
28. Kim YH, Park JW, Lee JY, Kwon TK. Sodium butyrate sensitizes TRAIL-mediated apoptosis by induction of transcription from the DR5 gene promoter through Sp1 sites in colon cancer cells. Carcinogenesis 2004;25:1813–20.
29. Nakata S, Yoshida T, Horinaka M, Shiraishi T, Wakada M, Sakai T. Histone deacetylase inhibitors upregulate death receptor 5/TRAIL-R2 and sensitize apoptosis induced by TRAIL/APO2-L in human malignant tumor cells. Oncogene 2004;23:6261–71.
30. Vanoosten RL, Moore JM, Karacay B, Griffith TS. Histone deacetylase inhibitors modulate renal cell carcinoma sensitivity to TRAIL/Apo-2L-induced apoptosis by enhancing TRAIL-R2 expression. Cancer Biol Ther 2005;4:1104–12.
31. Sonnemann J, Gange J, Kumar KS, Muller C, Bader P, Beck JF. Histone deacetylase inhibitors interact synergistically with tumor necrosis factor-related apoptosis-inducing ligand (TRAIL) to induce apoptosis in carcinoma cell lines. Invest New Drugs 2005;23:99–109.
32. Ling L, Cao Z, Goeddel DV. NF-κB-inducing kinase activates IKK-a by phosphorylation of Ser-176. Proc Natl Acad Sci U S A 1998;95:3792–7.
33. Yang J, Lin Y, Guo Z, et al. The essential role of MEKK3 in TNF-induced NF-κB activation. Nat Immunol 2001;2:620–4.
34. Arts J, de Schepper S, Van Emelen K. Histone deacetylase inhibitors: from chromatin remodeling to experimental cancer therapeutics. Curr Med Chem 2003;10:2343–50.
35. Blagosklonny MV, Robey R, Sackett DL, et al. Histone deacetylase inhibitors all induce p21 but differentially cause tubulin acetylation, mitotic arrest, and cytotoxicity. Mol Cancer Ther 2002;1:937–41.
36. Matsuyama A, Shimazu T, Sumida Y, et al. *In vivo* destabilization of dynamic microtubules by HDAC6-mediated deacetylation. EMBO J 2002;21:6820–31.
37. Roy S, Packman K, Jeffrey R, Tenniswood M. Histone deacetylase inhibitors differentially stabilize acetylated p53 and induce cell cycle arrest or apoptosis in prostate cancer cells. Cell Death Differ 2005;12:482–91.
38. Terui T, Murakami K, Takimoto R, et al. Induction of PIG3 and NOXA through acetylation of p53 at 320 and 373 lysine residues as a mechanism for apoptotic cell death by histone deacetylase inhibitors. Cancer Res 2003;63:8948–54.
39. Kovacs JJ, Murphy PJ, Gaillard S, et al. HDAC6 regulates Hsp90 acetylation and chaperone-dependent activation of glucocorticoid receptor. Mol Cell 2005;18:601–7.
40. Rahman MM, Kukita A, Kukita T, Shobuike T, Nakamura T, Kohashi O. Two histone deacetylase inhibitors, trichostatin A and sodium butyrate, suppress differentiation into osteoclasts but not into macrophages. Blood 2003;101:3451–9.
41. Yin L, Laevsky G, Giardina C. Butyrate suppression of colonocyte NF-κB activation and cellular proteasome activity. J Biol Chem 2001;276:44641–6.

42. Rundall BK, Denlinger CE, Jones DR. Combined histone deacetylase and NF-κB inhibition sensitizes non-small cell lung cancer to cell death. Surgery 2004; 136:416–25.
43. Mayo MW, Denlinger CE, Broad RM, et al. Ineffectiveness of histone deacetylase inhibitors to induce apoptosis involves the transcriptional activation of NF-κB through the Akt pathway. J Biol Chem 2003; 278:18980–9.
44. Leoni F, Zaliani A, Bertolini G, et al. The antitumor histone deacetylase inhibitor suberoylanilide hydroxamic acid exhibits antiinflammatory properties via suppression of cytokines. Proc Natl Acad Sci U S A 2002;99:2995–3000.
45. Quivy V, Van Lint C. Regulation at multiple levels of NF-κB-mediated transactivation by protein acetylation. Biochem Pharmacol 2004;68:1221–9.
46. Schmitz ML, Mattioli I, Buss H, Kracht M. NF-κB: a multifaceted transcription factor regulated at several levels. Chembiochem 2004;5:1348–58.
47. Roychowdhury S, Baiocchi RA, Vourganti S, et al. Selective efficacy of depsipeptide in a xenograft model of Epstein-Barr virus-positive lymphoproliferative disorder. J Natl Cancer Inst 2004;96:1447–57.
48. Dai Y, Rahmani M, Dent P, Grant S. Blockade of histone deacetylase inhibitor-induced RelA/p65 acetylation and NF-κB activation potentiates apoptosis in leukemia cells through a process mediated by oxidative damage, XIAP down-regulation, and c-Jun N-terminal kinase 1 activation. Mol Cell Biol 2005;25: 5429–44.
49. Adam E, Quivy V, Bex F, et al. Potentiation of tumor necrosis factor-induced NF-κB activation by deacetylase inhibitors is associated with a delayed cytoplasmic reappearance of IκBα. Mol Cell Biol 2003; 23:6200–9.

# Histone Deacetylase Inhibitors Suppress the Inducibility of Nuclear Factor- κB by Tumor Necrosis Factor-α Receptor-1 Down-regulation

Gabriele Imre, Volker Gekeler, Astrid Leja, et al.

*Cancer Res* 2006;66:5409-5418.